Open Access

Surface Wave Discharges Generated with Ar/He and Ar/N_2 Gas Mixtures at Atmospheric Pressure

José Muñoz, José Antonio Bravo and María Dolores Calzada*

Grupo de Espectroscopia de Plasmas, Edificio Einstein, Campus Rabanales. Universidad de Córdoba, 14071 Córdoba, Spain

Abstract: This work is aimed at studying emission spectra and morphological characteristics of surface wave discharges generated with Ar/He and Ar/N_2 gas mixtures at atmospheric pressure with powers ranging from 80 to 400 W. In both cases, power density is higher than that found with pure Ar, although these changes are due to different discharge features. Kinetic processes can be derived from the analysis of plasma-emitted spectra. We also provide evidence of variations in the external aspect of discharges (filamentation and contraction) related to changes in thermal conductivity in gas mixture.

Keywords: Surface wave discharges, atmospheric pressure, argon, helium, nitrogen, plasma kinetics.

INTRODUCTION

Throughout the last years, plasmas operated at atmospheric pressure have been object of increased attention due to their potential and current use in varied applications such as excitation for elemental analysis [1-3] and, more recently, medical instrument sterilization [4]. To ensure that industrial and technological applications of plasmas are carried out with maximum effectiveness, it is necessary to get to know the main factors (parameters) which determine discharge's ability to induce certain microscopic processes (discharge kinetics). This ability depends on the densities (populations) of the different plasma species contained in discharge and the energy available therein (temperatures).

Microwave induced plasmas (MIPs), and especially surface-wave sustained discharges, have proven to be an interesting tool in multiple fields such as sample analysis [5], noble gas purification [6] or sterilization [4]. This work carries out a preliminary study on spectroscopic and morphological differences of atmospheric-pressure Ar/He and Ar/N_2 surface-wave discharges (SWDs).

SURFACE WAVE DISCHARGES

In SWDs an electromagnetic wave is excited at a certain point of a plasma column by means of a wave launcher and propagated mainly by the plasma-dielectric interface [7]. In these discharges, plasma plays a dual role, acting simultaneously as an element which absorbs the microwave power carried by the wave and as a support for wave propagation. Thus, surface wave creates the plasma necessary for propagation by dissipating the power it carries.

Surface wave discharges are characterized by an electron-density decrease in plasma column from the exciter (the area where HF power is supplied) towards the end of the discharge. This end is determined by a particular critical electron density. Below this value, the surface wave cannot propagate due to a sharp increase in the attenuation coefficient (low pressure discharges) or the lack of power necessary to produce new ionizations (atmospheric pressure discharges). Therefore, the plasma column shows a well-defined length which obviously increases as power supplied to the discharge increases.

Another important parameter in SWDs is power linear density (L), defined as the power absorbed (P_{abs}) per unit of length, which provides information about the energy transferred from the wave to the discharge [8-10]. So, L is considered to be an estimation of the energy available in the discharge, the processes (kinetics) taking place within it depending on this energy. On the other hand, in surface wave discharges at atmospheric pressure generated with pure gas, it is well known that electrons control internal plasma kinetics (excitation/ionization) [10], which shows a close relation to the L value [9, 10]. According to theoretical studies on SWDs [8], linear power density appears as a fundamental modelling parameter to determine spatial structure in the plasma column. From an experimental point of view, the L value in a surface wave discharge can be obtained from the ratio between the power absorbed (P_{abs}) by the discharge and plasma-column length (l) [11]. Thus, L values calculated in this way should be considered average values for plasma columns designed by $\bar{L}$.

Finally, these discharges present the effect of radial contraction, characterized by the glowing region of the discharge receding from the tube wall. Due to this effect, in surface wave discharges two or more filaments can appear depending on operating conditions (plasma gas and discharge tube radius) [11]. This phenomenon may have detrimental effects in some applications; for instance, in microwave light sources [12] and gas treatment processes [6].

EXPERIMENTAL SETUP

Fig. (**1**) shows a schematic block diagram of plasma source as well as of optical detection and data collection sys-

*Address correspondence to this author at the Grupo de Espectroscopia de Plasmas, Edificio Einstein, Campus Rabanales. Universidad de Córdoba, 14071 Córdoba, Spain; E-mail: fa1cazal@uco.es

tems for the emission spectroscopy measurements used in experimentation.

Microwave power to plasma was provided by a SAIREM 12kT/t microwave generator of 2000 W maximum power in continuous mode equipped with a water-cooled circulator to avoid power reflection damage. Power was coupled to plasma by a surfaguide [13] with values ranging from 100 to 400 W in continuous mode.

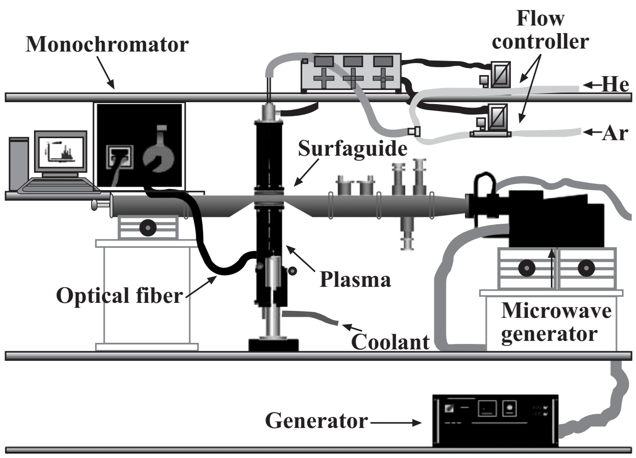

Fig. (1). Experimental device.

By means of two impedance matching systems of the wave launcher, the power reflected from the applicator back to the generator is made to be lower than 5 % of incident power.

The discharge was contained in quartz tubes with different inner and outer radii (2 and 3 mm). It is well known that a 12 cm-long microwave Ar plasma column can be sustained by using 200 W. Nonetheless, for a pure He discharge of about 5 cm, the application of up to 1400 W becomes necessary. Since the quartz tube containing the discharge undergoes a great deal of damage for powers over 300 W, it was cooled. For this reason, the discharge tube was coaxially surrounded by another quartz tube with 8.5 mm of internal radius as a jacket through which a dielectric liquid circulated. In our experiments, the plasma column extended to both sides of the wave launcher resulting in the appearance of direct and inverse columns [14]. A direct column is considered to be one where gas flux and wave propagation take place in the same direction, contrary to those in inverse column.

Several gas mixtures of high purity (99.999 %) Ar, He and N_2 were used as plasma gases with different total flows equal to 0.5 and 1 slm for Ar/He mixtures, and 1 and 2 slm for Ar/N_2 mixtures. Total flows were kept unchanged for a given set of measurements to ensure comparability. Gas flows were controlled by HI-TEC flow controllers (IB 31) with different maximum flow limits (0.25 and 5 slm).

An optical fibre was used to drive the light emitted from the discharge into a Jobin-Yvon-Horiba monochromator previously calibrated and equipped with a 2400-grooves/mm holographic grating. A Symphony CCD was used as a radiation detector. In order to carry out the study proposed, spectra within the visible 300-730 nm range were registered.

Together with the spectra, some photographs of the discharges were taken to account for variations in discharge morphology. Due to plasma intense brightness, a filter was employed to attenuate and avoid saturation of the digital camera.

RESULTS AND DISCUSSION

Linear Power Density ($\bar{L}$)

As stated before, linear power density L is a very important parameter in SWDs [8-10], since it somehow determines the amount of energy effectively transferred from the electromagnetic field into the discharge and thus the energy available for the different processes taking place in it.

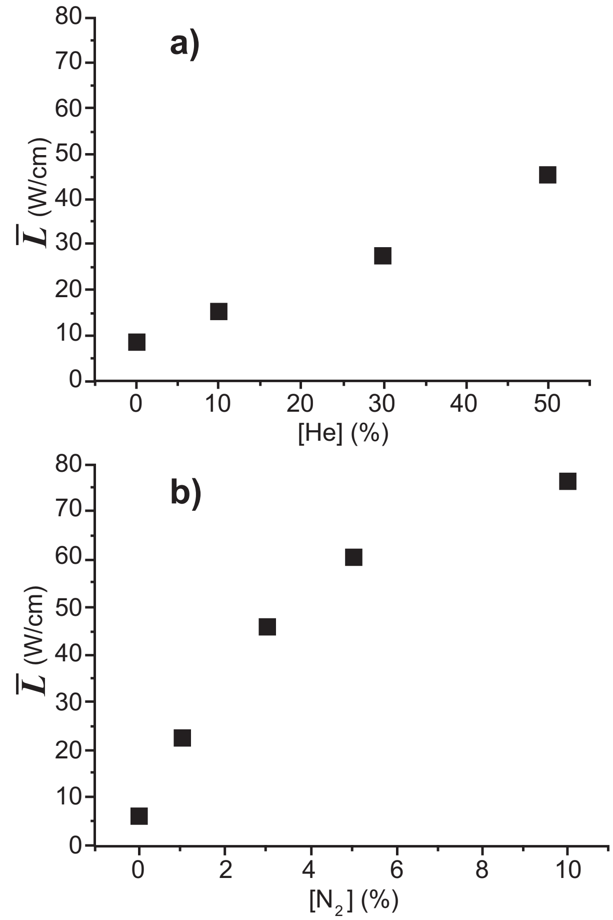

Fig. (2). Estimated linear power density ($\bar{L}$) *vs* He (**a**) and N_2 (**b**) concentration.

An estimation of L was calculated for both Ar/He and Ar/N_2 discharges following the procedure indicated in the previous section. As it can be seen in Fig. (**2**), the addition of either He or N_2 increases the value of $\bar{L}$ due to a simultaneous reduction in discharge length and increase in power demands necessary to sustain discharges. This increase is more significant when N_2 is added to an Ar discharge.

It is important to note that, for plasma generated with pure gas, an increase in $\bar{L}$ is correlated to an increase in excitation processes and, consequently, in greater intensities found in plasma-emitted spectral lines. However, the addition of He or N_2 to an Ar SWD involves an increase of $\bar{L}$ but also an intensity decrease in lines emitted by the plasmas under study.

Atomic and Molecular Emission Spectroscopy

In Ar/He plasma, some He I or even Ar II lines would be likely to appear in the spectra after the addition of a certain amount of He to pure Ar discharge. However, the only remarkable effect observed was a decrease in Ar I line intensities, as it can be seen in Figs. (**3a-c**).

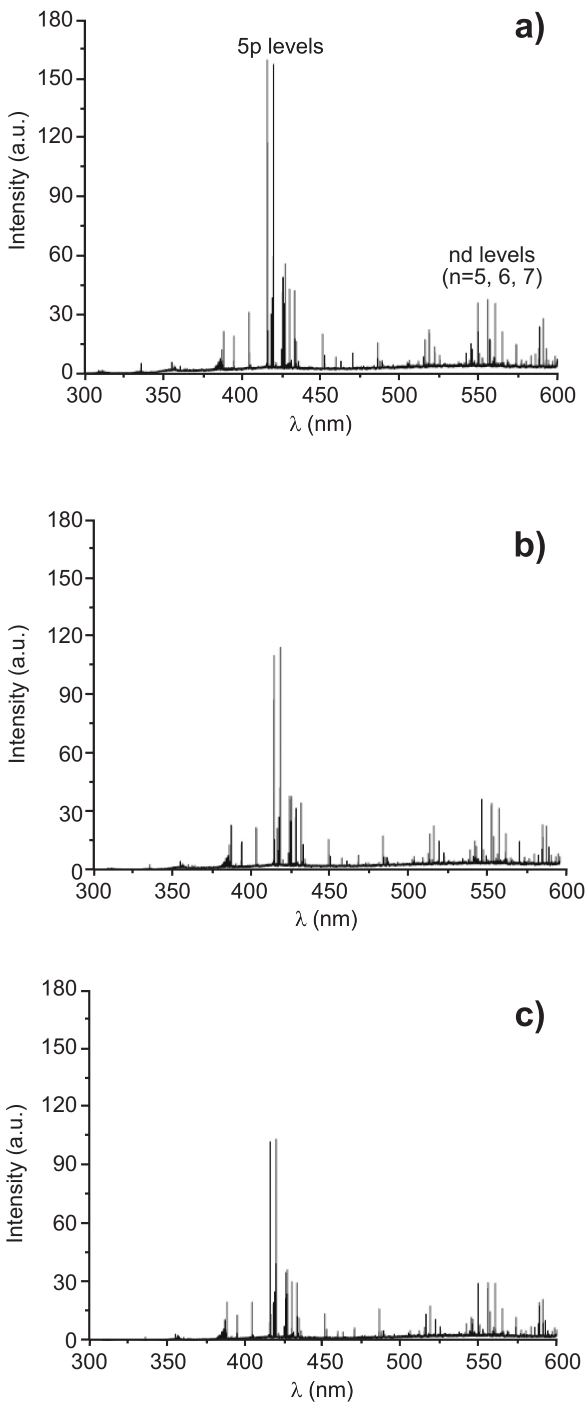

Fig. (3). Spectra of an Ar/He discharge recorded in the 300-600 nm region for different He concentration: 0 % (**a**), 10 % (**b**) and 30 % (**c**).

At atmospheric pressure, excitation and ionization processes are carried out stepwise, the atoms' metastable level being the starting level. Consequently, electrons belonging to the EEDF bulk take part in excitation and ionization processes in this metastable level. From the spectra shown in Figs. (**3a-c**), it can be deduced that the energy of great part of discharge fast-electrons is below 19.7 eV (He mestastable energy) and the density of He atoms in metastable state is lower than that of Ar atoms in such state (11.6 eV). On the other hand, it is known that the effective cross-section for momentum transfer of He is larger than that of Ar for a wide range of electron temperatures [15, 16]. Consequently, discharge energy is partly lost in elastic electron collisions with He atoms. As a global result, the energy available for Ar excitation and ionization diminishes and the excitation/ionization chain of processes is altered, resulting in a lower amount of excited Ar atoms.

On the other hand, when N_2 is added to the discharge, new species appear even at N_2 concentrations as low as 1 % such as molecular bands belonging to excited molecules (N_2) and molecular ions (N_2^+) as well as other bands belonging to excimers such as *CN*. Table **1** summarizes the molecular emissions found when analyzing the spectra shown in Figs. (**4a-c**).

Table **2** shows the energies of the different states corresponding to N_2 molecules and N_2^+ ion. Contrary to what happens in Ar/He mixtures, some reactions between Ar and N_2 are energetically favourable (Table **2**), particularly Reactions (1) and (2) corresponding to Penning excitation and charge transfer, respectively [17, 18].

$$Ar^m + N_2\left(X^1\Sigma_g^+\right) \rightarrow Ar^0 + N_2\left(C^3\Pi_u\right) \quad (1)$$

$$Ar^+ + N_2\left(X^1\Sigma_g^+\right) \rightarrow Ar^0 + N_2^+\left(X^2\Sigma_g^+\right) \quad (2)$$

Table 1. List of Molecular Bands Observed in Ar/N_2 Mixtures

Molecule	Transition	Spectral Interval (nm)
N2	$N_2\left(B^3\Pi_g\right) \rightarrow N_2\left(A^3\sum_u^+\right)$ First positive system	503-730
	$N_2\left(C^3\Pi_u\right) \rightarrow N_2\left(B^3\Pi_g\right)$ Second positive system	330-500
N2+	$N_2^+\left(B^2\Sigma_u^+\right) \rightarrow N_2^+\left(X^2\Sigma_g^+\right)$ First positive system	380-392 420-428
CN	$CN\left(B^2\Pi\right) \rightarrow CN\left(A^2\Sigma\right)$ Violet System	335-360 373-389

Furthermore, other reactions are intermediate excited molecular states which can be reached by means of direct or stepwise electron excitation (3-5) [19, 20].

$$N_2\left(X^1\Sigma_g^+\right) + e^- \rightarrow N_2\left(C^3\Pi_u\right) + e^- \quad (3)$$

$$N_2\left(X^1\Sigma_g^+\right) + e^- \rightarrow N_2\left(A^3\Sigma_u^+\right) + e^- \quad (4)$$

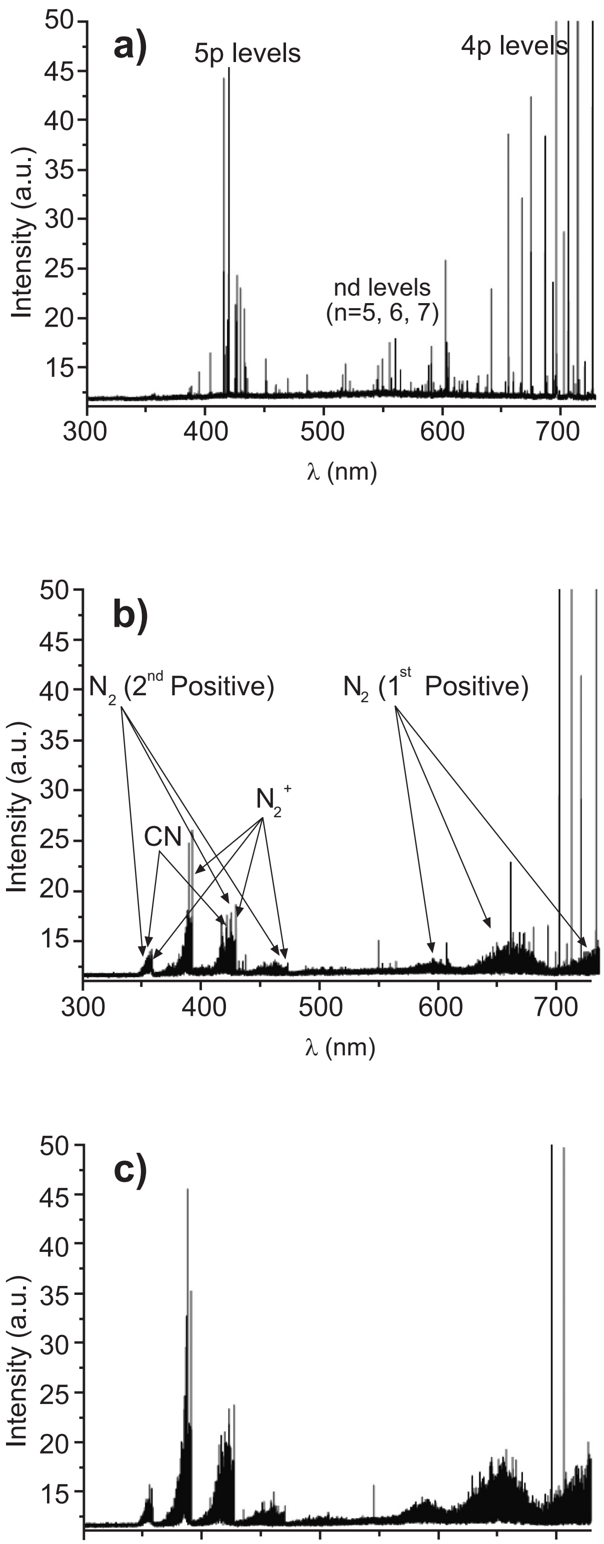

Fig. (4). Spectra of an Ar/N_2 discharge recorded in the 300-730 nm region for different N_2 concentration: 0 % (**a**), 1 % (**b**) and 5 % (**c**).

$$N_2\left(A^3\Sigma_u^+\right)+e^- \rightarrow N_2\left(C^3\Pi_u\right)+e^- \quad (5)$$

Table 2. List of N_2 Excited Molecules and Molecular Ions

Species	Excitation Energy (eV)
$N_2\left(A^3\Sigma_u^+\right)$	6.17
$N_2\left(B^3\Pi_g\right)$	7.35
$N_2\left(C^3\Pi_u\right)$	11.03
$N_2^+\left(X^2\Sigma_g^+\right)$	15.58
$N_2^+\left(A^2\Pi_u\right)$	16.73
$N_2^+\left(B^2\Sigma_u^+\right)$	18.75
$N_2^+\left(D^2\Sigma_g\right)$	22.00

While charge transfer reactions (2) do not contribute to a net loss of electrons, the remainder processes may involve partial energy loss in electron energy distribution function (EEDF) towards the electronic excited states of N_2 molecules (3-5). Particularly, Reaction (1) may lead to a decrease in metastable Ar density and, consequently, to a population decrease in Ar excited levels. Additionally, a part of the energy ceded to the discharge is stored in the rovibrational state of N_2 molecules.

This fact is illustrated in Figs. (**5**, **6**). As nitrogen concentration in the discharge increases from 0 to 10 %, the emission intensity of the band-head of both N_2 (First Positive System) and N_2^+ (First Negative System) increases as a result of population increases in $N_2(B^3\Pi_g)$ and $N_2^+(B^2\Sigma_u^+)$ species, respectively; while the intensity of the Ar 727.7 nm line sharply decreases.

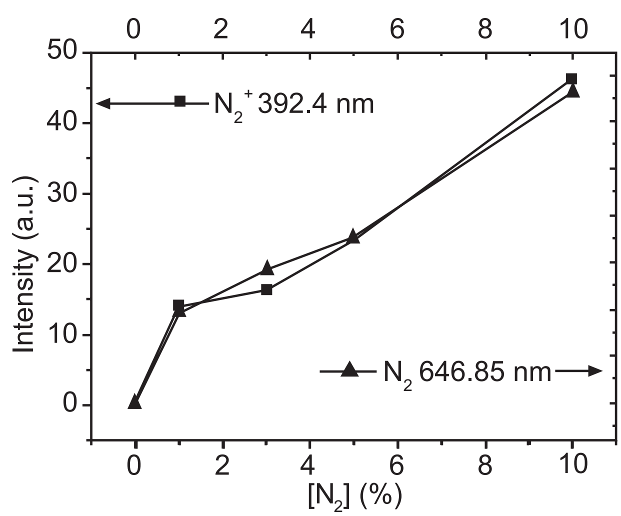

Fig. (5). Intensity variation, with respect to N_2 concentration, of 392.4 and 646.85 nm bandheads of the First Positive System of N_2 and the First Negative System of N_2^+, respectively.

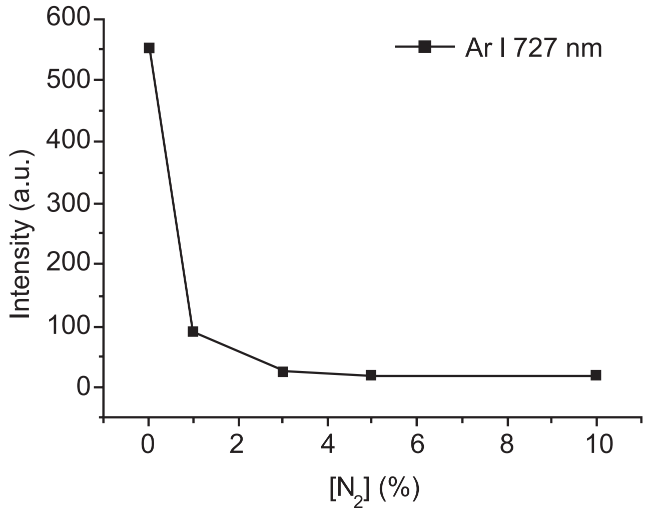

Fig. (6). Intensity variation, with respect to the N_2 concentration, of the peak height of the 727 nm Ar I line.

Even though an intense emission arising from the N_2 Second Positive System ($N_2(C^3\Pi_u) \rightarrow N_2(B^3\Pi_g)$) concerning Ar/N_2 discharges has been reported by some other publications [21, 22], it has also been detected in the discharge studied herein but only as a small signal mainly masked by the N_2^+ First Negative System in all cases.

This difference in the relative intensity of the Second Positive Systems and First Positive Systems of nitrogen suggests that molecular ions in the $X^2\Sigma_g^+$, $A^2\Pi_u$, $B^2\Sigma_u^+$ and $D^2\Pi_g$ electronically excited states can take part in a dissociative recombination reaction as that shown in (6) and thereafter contribute to the formation of the $B^3\Pi_g$ state of the nitrogen molecule through Reactions (7) or (8) [23].

$$N_2^+ + e^- \rightarrow N^0 + N^m \tag{6}$$

$$N^0 + N^m + Ar^m \rightarrow N_2\left(B^3D_g\right) + Ar^m \tag{7}$$

$$\begin{aligned} &N^0 + N^m + N_2\left(X^1\Sigma_g^+\right) \rightarrow \\ &\quad \rightarrow N_2\left(B^3D_g\right) + N_2\left(X^1\Sigma_g^+\right) \end{aligned} \tag{8}$$

Finally, knowing that none of the impurities contained in the gas used for discharge generation has CN dimmers, it becomes clear that free nitrogen atoms are also produced in plasma, although no atomic N lines have been detected.

Discharge Morphology and Contraction

Another effect of the introduction of He into the discharge is the disappearance of discharge contraction and filamentation (Fig. **7**). Both filaments on the inverse column slowly vanish as He concentration increases up to 30 %. Simultaneously, it can be seen how the column slowly widens to fill the whole section of the tube (highlighted detail in Fig. **7**). Both phenomena are a consequence of increase in discharge thermal conductivity [11].

Similarly, the addition of nitrogen to the Ar discharge has the same effect on discharge contraction and filamentation (Fig. **8**) also due to an increase in thermal conductivity. Moreover, other consequences on the external aspect of the discharge can be observed. Two areas can be well-distinguished at N_2-concentrations as low as 1 % in the discharge. The first, a bright one, is the discharge itself, while the second, much more diffuse, corresponds to postdischarge, in which the emissions of long-lived N_2 molecules can be detected (highlighted detail in Fig. **8**).

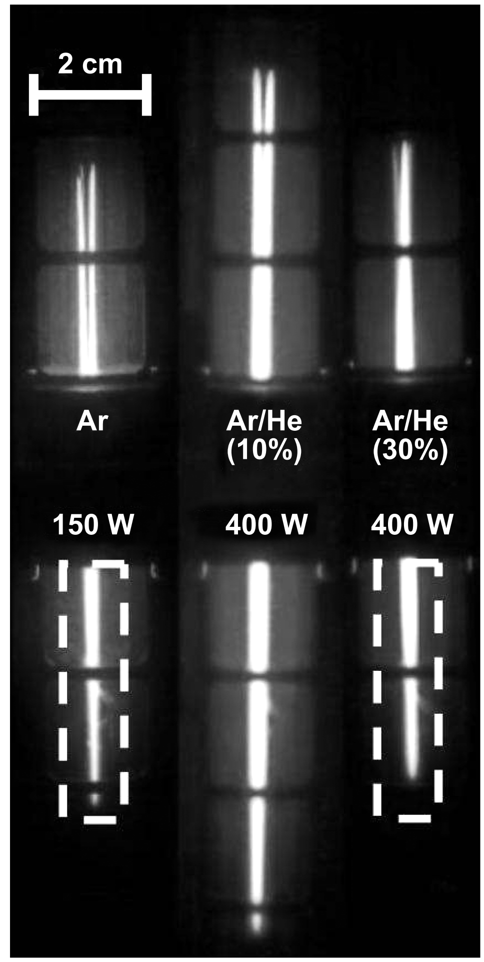

Fig. (7). Photographs taken from SWD for different Ar/He discharges.

CONCLUSIONS

Differences in the excitation mechanisms of Ar/He and Ar/N_2 SWDs have been determined by a spectroscopic study of discharge up to a concentration of 30 and 10 %, respectively.

In Ar/He discharges, it has been found that He atoms act as an energy sink for EEDF through elastic collisions due to their higher collision cross-section for momentum transfer, perturbing the excitation/ionization chain of Ar processes.

On the other hand the role of nitrogen molecules in Ar/N_2 SWDs is quite different. Due to the existence of excited molecular states below the energy of Ar metastable atoms and closer to the typical energies of the electrons within EEDF, nitrogen molecules are effectively excited by Penning excitation, charge transfer or through electron inelastic collisions.

Discharge contraction and filamentation have been shown as well as discussed for both Ar/He and Ar/N_2 mixtures. The disappearance of both phenomena with an increasing proportion of both He and N_2 indicates an increase in thermal conductivity.

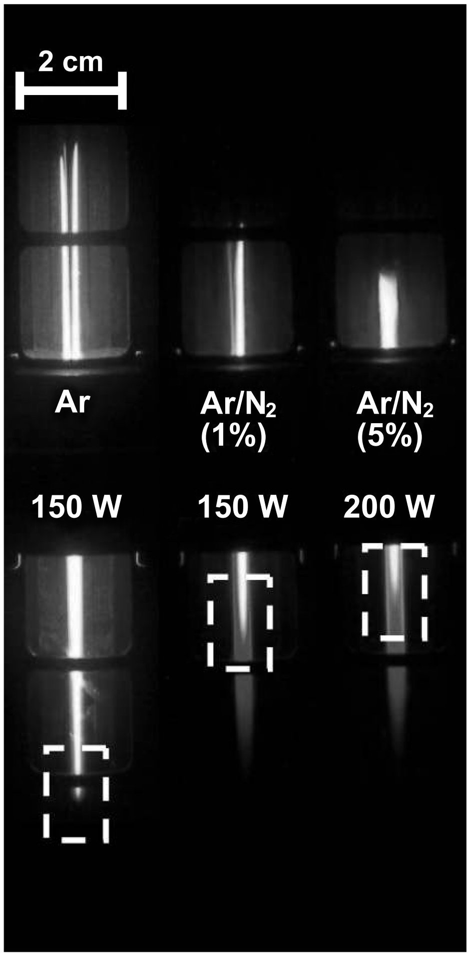

Fig. (8). Photographs taken from SWD for different Ar/N$_2$ discharges.

ACKNOWLEDGEMENT

This work was supported by the Spanish Ministry for Education and Science under contract No ENE 2005-00314 and FEDER funds (European Union).

REFERENCES

[1] Montaser A. Inductively Coupled Plasmas in Analytical Atomic Spectrometry. 2nd ed. New York VCH 1992.

[2] Wagatsuma K. Emission characteristics of mixed gas plasmas in low-pressure glow discharges. Spectrochim Acta B 2001; 56: 465-86.

[3] Sun F, Sturgeon RE. Furnace atomization plasma emission spectrometry with He/Ar mixed gas plasmas. Spectrochim Acta B 1999; 54: 2121-41.

[4] Moisan M, Barbeau J, Crevier MC, Pelletier J, Phillip N, Saoudi B. Plasma Sterilization. Methods Mech Pure Appl Chem 2002; 73: 349-58.

[5] Tran KC, Lauzon C, Sing R, Hubert J. Non-metal atomic emission spectrometry in helium surface-wave sustained plasmas at 40 and 2450 MHz. J Anal At Spectrom 1998; 13: 507-13.

[6] Kabouzi Y, Moisan M, Rostaing JC, *et al*. Abatement of perfluorinated compounds using microwave plasmas at atmospheric pressure. J Appl Phys 2003; 93: 9483-96.

[7] Zakrzewski Z, Moisan M, Sauvé G. Microwave Excited Plasmas. Amsterdam: Elsevier 1992.

[8] Nowakowska H, Zakrzewski Z, Moisan M, Lubánski M. Propagation characteristics of surface waves sustaining atmospheric pressure discharges: the influence of the discharge processes. J Phys D Appl Phys 1998; 31: 1422-32.

[9] Calzada MD, Sáez M, García MC. Characterization and study of the thermodynamic equilibrium departure of an argon plasma flame produced by a surface-wave sustained discharge. J Appl Phys 2000; 88: 34-39.

[10] Calzada MD, García MC, Luque JM, Santiago I. Influence of the thermodynamic state in the excitation of samples by a plasma at atmospheric pressure. J Appl Phys 2002; 92: 2269-75.

[11] Kabouzi Y, Calzada MD, Moisan M, Tran KC, Trassy C. Radial contraction of microwave-sustained plasma columns at atmospheric pressure. J Appl Phys 2002; 91: 1008-19.

[12] Kudela J, Odrobina I, Kando M. High-speed camera study of the surface wave discharge propagation in xenon. Jpn J Appl Phys 1998; 37: 4169-76.

[13] Moisan M, Etemadi E, Rostaing JC, French Patent No. 2 762 748 (1998), European Patent No EP 0 874 537 A1 (1998).

[14] Martínez-Aguilar J, Castaños-Martínez E, García MC, Calzada MD. Proceedings on the XXVIII Internacional Conference on Plasma and Ionized Gases; Prague, Czech Republic 2007.

[15] Sainz A. PhD Thesis. Universidad de Córdoba 2006; pp. 123-48.

[16] Raju GG. Gaseous Electronics: Theory and Practice. Boca Ratón: Taylor & Francis 2006; pp. 93-192.

[17] Ricard A. Reactive Plasmas. Paris: Société Française du Vide 1996; pp. 55-88.

[18] Tatarova E, Dias FM, Henriques J, Ferreira CM. Large-scale Ar and N-2-Ar microwave plasma sources. J Phys D Appl Phys 2006; 39: 2747-53.

[19] Petitjean L, Ricard A. Emission-spectroscopy study of N-2-H-2 glow-discharge for metal-surface nitriding. J Phys D Appl Phys 1984; 17: 919-29.

[20] Qayyum A, Zeb S, Ali S, Waheed A, Zakaullah M. Optical emission spectroscopy of abnormal glow region in nitrogen plasma. Plasma Chem Plasma Process 2005; 25: 551-64.

[21] Ricard A, Czerwiec T, Belmonte T, Bockel S, Michel H. Detection by emission spectroscopy of active species in plasma-surface processes. Thin Solid Film 1999; 341: 1-8.

[22] Qayyum A, Zeb S, Naveed MA, Rehman NU, Ghauri SA, Zakaullah M. Optical emission spectroscopy of Ar-N2 mixture plasma. J Quant Spectrosc Radiat Transf 2007; 107: 361-71.

[23] Ricard A, Deschamps J, Godard JL, Falk L, Michel H. Nitrogen-atoms in Ar-N2 flowing microwave discharges for steel surface nitriding. Mater Sci Eng A 1991; 139: 9-14.

Received: March 31, 2008 Revised: March 3, 2009 Accepted: March 3, 2009